

# UCSF

## UC San Francisco Previously Published Works

### Title

HER2 amplification in tumors activates PI3K/Akt signaling independent of HER3

### Permalink

<https://escholarship.org/uc/item/3nt8x4zs>

### Journal

Cancer Research, 78(13)

### ISSN

0008-5472

### Authors

Ruiz-Saenz, Ana  
Dreyer, Courtney  
Campbell, Marcia R  
[et al.](#)

### Publication Date

2018-07-01

### DOI

10.1158/0008-5472.can-18-0430

Peer reviewed



Published in final edited form as:

*Cancer Res.* 2018 July 01; 78(13): 3645–3658. doi:10.1158/0008-5472.CAN-18-0430.

## HER2 amplification in tumors activates PI3K/Akt signaling independent of HER3

Ana Ruiz-Saenz, Courtney Dreyer, Marcia R Campbell, Veronica Steri, Nate Gulizia, Mark M Moasser\*

Department of Medicine, Helen Diller Family Comprehensive Cancer Center, University of California, San Francisco, San Francisco, CA 94143

### Abstract

Current evidence suggests that HER2-driven tumorigenesis requires HER3. This is likely due to the unique ability of HER3 to activate PI3K/Akt pathway signaling, which is not directly accessible to HER2. By genetic elimination of HER3 or shRNA knockdown of HER3 in HER2-amplified cancer cells, we find residual HER2-driven activation of PI3K/Akt pathway signaling that is driven by HER2 through direct and indirect mechanisms. Indirect mechanisms involved second messenger pathways including Ras or Grb2. Direct binding of HER2 to PI3K occurred through p-Tyr1139, which has a weak affinity for PI3K but becomes significant at very high expression and phosphorylation. Mutation of Y1139 impaired the tumorigenic competency of HER2. Total elimination of HER3 expression in HCC1569 HER2-amplified cancer cells significantly impaired tumorigenicity only transiently, overcome by subsequent increases in HER2 expression and phosphorylation with binding and activation of PI3K. In contrast to activation of oncogenes by mutation, activation by overexpression was quantitative in nature: weak intrinsic activities were strengthened by overexpression, with additional gains observed through further increases in expression. Collectively, these data show that progressive functional gains by HER2 can increase its repertoire of activities such as the activation of PI3K and overcome its dependency on HER3.

### Keywords

HER2; HER3; Neu; breast cancer; HER2 amplification

### Introduction

Amplification and overexpression of HER2 is seen in a subset of cancers including more than 20% of breast cancers. A considerable body of experimental evidence strongly suggests that HER2 is the oncogenic driver of these cancers, important in the genesis and progression of these tumors (reviewed in (1,2)). HER2 belongs to a homologous family of receptor tyrosine kinases (RTKs) that include EGFR, HER3, and HER4 (reviewed in (3)).

**Corresponding Authors:** Mark M. Moasser, MD, Box 1387, University of California, San Francisco, San Francisco, CA 94143-1387, Tel: 415-476-0158, Fax: 415-353-9592, mark.moasser@ucsf.edu, Ana Ruiz-Saenz, PhD, Box 1387, University of California, San Francisco, San Francisco, CA 94143-1387, Tel: 415-476-0685, ana.ruiz-saenz@ucsf.edu.

\*lead contact

Cooperation manifest as heterodimerization and transphosphorylation is a key feature of HER family signaling. Although these receptors are highly homologous in their extracellular ligand-binding and intracellular kinase domains, they are divergent in their intracellular c-terminal signaling tails. This allows for signaling via diverse effector pathways depending on the precise repertoire of HER family members expressed in a certain cell type and phosphorylated through heterodimerization events initiated by specific ligands. In particular, HER3 is uniquely endowed with 6 consensus binding site phosphotyrosines for the recruitment of the SH2 domain of the regulatory subunit of PI3K, and is a potent activator of PI3K when phosphorylated (4,5). Although EGFR and HER4 can directly or indirectly bind and activate PI3K (6,7), the transmission of the signaling down the PI3K/Akt pathway of HER family members is typically thought to be mediated through the transphosphorylation of HER3.

As the role of the PI3K/Akt pathway in regulating numerous cellular processes paramount for tumorigenic growth has become more and more recognized, so has the role of HER3 as an upstream driver of this pathway. Experimental studies of the past decade have identified HER3 as a critical partner for HER2 in the genesis and progression of HER2-amplified cancers. Several knockdown or gene deletion models show that HER2-driven tumors do not develop or grow in the absence of HER3 expression (8–10). Naturally, this requirement for HER3 has been attributed to its potent ability to activate PI3K pathway signaling, which is critical for tumorigenic growth, and which HER2 is thought unable to directly activate.

We have been interested in developing deeper insights into the role of HER3 in HER2-amplified cancers. In particular, we have been interested in understanding why HER3 is required, whether the requirement is for the activation of PI3K, and whether its requirement is absolute or perhaps conditional or transient. This question is of paramount importance, as much effort is currently being placed into the development of HER3 inhibitors to complement HER2 inhibitors, and it would be of much value to know whether this will constitute the endgame in the treatment of HER2-amplified cancers, or whether it will provide benefits that are incremental in nature. Towards this cause, we engineered the loss of HER3 expression in HER2-amplified cancer cells and studied the resulting phenotypic consequences. The immediate findings show the loss of tumorigenic growth, confirming previous reports. But this appears to be a transient phenotype, and increased HER2 expression and autophosphorylation ultimately supplants the requirement for HER3 and restores tumorigenic growth in a HER3-independent manner.

## Materials and Methods

**Cells and reagents**—Cell lines (BT474, SkBr3, HCC1569, CHO-K1 and MCF10A) were obtained from the American Type Culture Collection (ATCC). Authentication was performed using DNA Diagnostics Center (Fairfield, OH). Cells were cultured at 37°C in a 95% air/5% CO<sub>2</sub> atmosphere. Cells were grown in Dulbecco's Modified Eagle's Medium (DMEM)/HamF12 media (BT474 and SkBr3), RPMI 1640 media (HCC1569) or F-12K (CHO-K1) supplemented with 10% fetal bovine serum, penicillin, streptomycin, and L-glutamine. MCF10A cells were grown in DMEM/HamF12 media containing 5% horse serum, 10ug/ml insulin, 0.5ug/ml hydrocortisone, 20ng/ml EGF, penicillin, streptomycin,

and L-glutamine. NR6 cells were grown in DMEM high glucose containing 10% fetal bovine serum, sodium pyruvate, non-essential aminoacids, 10mM HEPES buffer, penicillin, streptomycin, and L-glutamine. Conditioned medium from cell lines was routinely checked for mycoplasma contamination by PCR using the primers: 5' – GGG AGC AAA CAG CAT TAG ATA CCC – 3' and 5' – TGC ACC ATC TGT CAC TCT GTT AAC CTC – 3'. Cells were used after a low number of passages (2 to 4) after thawing. Lapatinib was purified from commercial Tykerb tablets by organic extraction as previously described (11). GDC-0941 and BEZ235 were purchased from Selleckchem. Methyl Cellulose was purchased from Sigma (#M0262–250G). Matrigel® Basement Membrane Matrix was purchased from Corning (Phenol Red-Free #356237).

**DNA construction**—The HER2 mutants were generated at Genewiz and all mutated vectors were confirmed by sequencing the entire cDNA insert. The Tyr 1143 to Phe mutation in NeuT was introduced using the Stratagene site-directed mutagenesis kit and protocol with the following complementary primers; the sense primer was 5'-CCCAGCCCCGAGTTTGTGAACCAATC-3', while the anti-sense primer was 5'-GATGGTTCACAACTCGGGCTGGG-3'. For expression in CHO-K1 cells, HER2 wt and mutant cDNAs were HA tagged at the C-terminus and subcloned into the same mammalian expression vector. For expression in the MCF-10A cells, both NeuT and NeuTY1143F mutant were flag tagged at the C-terminus and subcloned into the same retroviral vector. Plasmids used are as follows. Gene expression in NR6 cells and MCF10A was done using the retroviral pMSCV PIG vector (gift of David Bartel, addgene #21654). Human p85 expression in CHO-K1 cells was done using pSV-human p85 $\alpha$  (gift of Ronald Kahn, addgene #11499). HER2 mutant expression in CHO-K1 cells was done using the pDEST40 plasmid vector (ThermoFisher).

**Cell transfection, retrovirus production and production of stable cell lines**—siRNA and plasmid transfections were performed using Lipofectamine 2000 according to the manufacturer's instructions (Invitrogen). Cells were processed 24 or 72 hours after plasmid or siRNA transfection, respectively. siRNAs Control and targeting H-Ras, N-Ras, K-Ras, EGFR and Grb2 were obtained from Dharmacon. Cells transfected with control siRNAs were used as controls in all experiments.

For inducible knockdowns of HER3, the oligonucleotides were synthesized and annealed and then ligated into the pSuperior vector. Standard protocols were used according to the manufacturers (OligoEngine). shRNA sequences used are described below:

5'-  
GATCCCAAGAGGATGTCAACGGTTATTCAAGAGATAACCGTTGACATCCTCTTTTT  
TTA-3'

5'-  
AGCTTAAAAAAGAGGATGTCAACGGTTATCTCTTGAATAACCGTTGACATCCTCT  
TGG-3'

The NR6 and MCF-10A cell lines stably expressing HER2, NeuT or NeuTY1143F proteins were produced by infection with respective retroviruses in the presence of 1 µg/ml polybrene (Sigma). After incubation in growth medium for approximately 48 hours, cells were treated with 1 µg/ml puromycin, the selection antibiotic expressed by the viral vector, to remove non-expressing cells. Puromycin-resistant cell populations were used for the various experiments described in the relevant sections.

For HCC1569 HER3KO cells generation, CRISPR/Cas9 KO plasmids of HER3 (h, sc-400146) were used to generate stable HER3 knockout HCC1569 cells according to manufacturer's instructions. Either individual or pooled single cell clones with efficient target gene KO (as indicated in Figures) were used for downstream functional experiment to minimize the clonal variation

**Antibodies and western blotting**—Cell and tumor lysates were prepared using modified RIPA lysis buffer (150 mM NaCl, 0.1% SDS, 1% Nonidet P40, 1% sodium deoxycholate and 10 mM sodium phosphate, pH 7.2) supplemented with protease and phosphatase inhibitors. Tumor lysates were briefly sonicated to break chromosomal DNA that could interfere with polyacrylamide gel electrophoresis separation of proteins. After clearing by centrifugation at 12,000 rpm for 10 minutes, the lysates were analyzed as described in the respective experiments. For electrophoresis gel separation of proteins, samples were denatured by boiling with Laemmli sample buffer and run on an 8% denaturing polyacrylamide gel. After transfer onto a nitrocellulose membrane and blocking with 3% bovine serum albumin, the membranes were stained with primary antibodies overnight at 4 °C, washed 3 times with TBST (Tris-buffered saline containing 1% Triton-X-100), stained with secondary antibodies for 1 hour at room temperature and detected using the chemiluminescence method. Western blots were performed using antibodies purchased from SantaCruz Biotechnologies (HER3 (5A12) #81455, actin #1616, vimentin (V9) #6260), Cell Signaling (EGFR #2232, p-HER2Y1248 #2247, p-HER2pY1221/Y1222 #2243, pAKT-Thr308 #4056, pAKT-Ser473 #4058, p-MAPK #9101, MAPK #9102, Ras #3965, Grb2 #3972), Abcam (p-HER2Y1139 #53290), Bethyl (p85b #A302–593A), and Millipore (p85a #05–212). Horseradish peroxidase-conjugated secondary antibodies were from Santa Cruz (mouse and goat) and GE Healthcare, (rabbit).

Phospho-RTK profiling was done with the RayBio C-Series Phospho-RTK Antibody Array according to manufacturer's instructions. Briefly, the array membranes were blocked in blocking buffer and incubated with diluted cell lysates overnight at 4C. After washing, the array membranes were incubated with the detection antibody, washed again, and developed with standard chemiluminescent reagents.

**qPCR**—Total cellular RNA was isolated using the Qiagen RNeasy kit following the manufacturer's instructions. RT and PCR amplification of EGFR was performed using primers and methods that have been described previously (11). Quantitative PCR assays were performed for EGFR and the housekeeping gene  $\beta$ 2-microglobulin from cDNA prepared from different mouse cell lines and tissue. We used the  $C_T$  methodology to obtain the ratios after normalizing to  $\beta$ 2-microglobulin. The ratios were obtained against the

average for the positive control (cerebellum tissue). The mean ratio was determined on the duplicate values obtained.

**Anchorage-independent growth in soft agar**—Anchorage-independent growth in the soft agar was used as one of the assays to determine state of cell transformation. First, 6 cm cell culture plates were overlaid with 0.7% agar in the growth medium. Next,  $1 \times 10^4$  cells/well of control or overexpressing HER2 NR6 cells,  $1 \times 10^4$  cells/well of HCC1569-HER3WT or HCC1569-HER3KO in complete medium and  $5 \times 10^3$  cells/well of NeuT or NeuTY1143F-overexpressing MCF10A cells in medium without EGF and insulin, were suspended in 1.5 ml of growth medium mixed with melted agar to a final concentration of 0.4% and immediately poured onto the agar overlay. After 5 min of incubation at room temperature for the agar to solidify, the cells were transferred to a 37 °C and 5% CO<sub>2</sub> incubator. Colonies were counted after 10 days (MCF10A) or 21 days (Nr6 and HCC1569 cells) and pictures were taken using Quantity One software from Bio-Rad.

**Coimmunoprecipitation**—Cells serum starved overnight and treated with 1 $\mu$ M lapatinib or DMSO for 2 hours were scraped from the plate using RIPA (HCC1569 and BT474) or NP-40 (SkBr3) lysis buffer, incubated on ice for 30 min and centrifuged in a Minifuge for 5 min at 4 °C. The supernatant was used for the immunoprecipitation assay and a fraction of it as input. Lysates prepared from these cells were subjected to immunoprecipitation with 10  $\mu$ g of Herceptin coupled to proteinG-sepharose beads overnight at 4 °C., washed 3 times with lysis buffer, eluted by boiling for 5 min with Laemmli sample buffer, and analyzed by immunoblotting as described above.

**Animal experiments**—All mice studies were reviewed and approved by the UCSF Institutional Animal Care and Use Committee.  $2 \times 10^6$  HCC1569 cells (100  $\mu$ l, 1:1 matrigel: serum free RPMI) were implanted subcutaneously in female nude mice (Foxn1nu/Foxn1nu) at 6 to 8 weeks of age. For lapatinib treatment, when tumors reached a volume of 200mm<sup>3</sup>, HCC1569 HER3KO-bearing mice were randomly split into two groups. Mice were treated daily by oral gavage either with lapatinib (100mg/kg/day) or vehicle MCT control (0.5% w/v Methyl Cellulose, 0.2% v/v Tween 80).  $2 \times 10^6$  MCF10A cells (50  $\mu$ l, 1:1 matrigel: serum free RPMI) were implanted into the fourth mammary fat pad of female NSG mice (NOD-scid IL2Rgamma-null) at 6 to 8 weeks of age. Age-matched mice were assigned randomly to experimental groups. Biological replicates for each group are indicated by n in Figure legends. Tumor growth was assessed weekly by caliper measurement.

**Ki-67 staining:** Freshly harvested tumor tissue was fixed in 10% neutral buffered formalin phosphate for 24 hours at 4°C. Tumor tissue was paraffin-embedded and sectioned 4- $\mu$ m thick. For Ki-67 staining, paraffin tissue slides were heated in 60°C oven for 30 minutes, then deparaffinized by immersing the slides in xylene and rehydrating the tissue in 100% ethanol, 95% ethanol, 70% ethanol and deionized water washing steps (5 minutes each). Slides were subsequently immersed in 3% H<sub>2</sub>O<sub>2</sub> (in PBS) for 10 minutes to quench endogenous peroxidases. Both enzymatic and heat induced-antigen retrieval were performed as described: slides were immersed in pre-warmed 0.25% Trypsin (in PBS) for 15 minutes, washed in PBS for 5 minutes, then immersed in 10mM Citrate Buffer and heated in

microwave oven (900W) for 10 minutes. Slides were let cool down at room temperature for 30 minutes and blocked with 1.5% Normal Goat Serum (in PBS) for 30 minutes at room temperature. Slides were stained with monoclonal mouse  $\alpha$ -human Ki-67 Antigen antibody (1:200 in PBS 0.05% Tween-20; clone MIB-1, #M7240, Dako) overnight at 4°C. Following primary antibody incubation, slides were extensively washed in PBS. As secondary antibody, horse  $\alpha$ -mouse-biotinylated antibody 1:200 in PBS 0.05% Tween-20, #BA-2000, Vector Laboratories) was incubated for 30 minutes at room temperature followed by Vectastain Elite ABC HRP kit (#PK-6100, Vector Laboratories). Slides were washed in PBS and 3,3'-Diaminobenzidine tetrahydrochloride (DAB) Substrate (#D5905, Sigma) was added according to manufacturer's instructions. Nuclear hematoxylin counterstain was applied, followed by dehydration through 70% ethanol, 95% ethanol, 100% ethanol, and xylene (3 minutes each). Slides were mounted with Permount Mounting Medium (Fisher Scientific) and analysed on a bright-field microscope.

**Fluorescent in situ hybridization (FISH) for HER2**—FISH was performed using the PathVysion (Vysis Inc., USA) probe kit. In brief, tumor tissue was paraffin-embedded and sectioned 4- $\mu$ m thick. The section was air-dried, pretreated, and digested with proteinase K before being hybridized with fluorescent-labeled probes for the HER2 gene, and a-satellite DNA for chromosome 17. Nuclei were routinely counterstained with an intercalating fluorescent counterstain, DAPI. Tumors were imaged using a Spinning disk confocal Nikon TI inverted microscope ( $\times$ 60 objective, lasers 640, 488 and 561nm). For each tumor, at least 43 tumor cell nuclei were counted and scored for both HER2 and chromosome 17 centromere numbers.

**Quantification and Statistical Analysis**—For all analyses, significance was determined at  $p < 0.05$ . All analyses, unless specified elsewhere, were performed in GraphPad Prism® (GraphPad Software, Inc.). For analyses limited to two groups, Student's t-test was utilized. Data are expressed as mean  $\pm$  1 S.E.M., unless otherwise specified. For each experiment, unless otherwise noted, n represents the number of individual biological replicates.

## Results

### HER2-amplified cancer cells regrow following HER3 knockout

We have been interested in the role of HER3 in mediating HER2-driven tumorigenesis. Using CRISPR-Cas9 technology, we engineered the elimination of HER3 expression in HER2-amplified HCC1569 breast cancer cells. Three independent HER3 knockout (HCC1569-HER3KO) clones, confirmed to lack HER3 expression, were selected for further analysis (Figure 1A). Three clones that failed to undergo the gene targeting event and maintained HER3 expression were also selected as controls (HCC1569-HER3WT). HCC1569-HER3KO cells maintain their proliferative growth and can be maintained in continuous monolayer cell culture. In three dimensional culture conditions, both HCC1569-HER3WT and HCC1569-HER3KO formed solid acini although HER3 depletion significantly decreased the size and number of HCC1569-HER3KO acini, in agreement with previous studies (9) (Supplementary Figure S1 A,B). To determine the effect of HER3



function on tumorigenic growth, the three HCC1569-HER3WT and three HCC1569-HER3KO cells were implanted in nude mice. HCC1569-HER3WT cells generated tumors within 2 weeks and with a high take rate, whereas HCC1569-HER3KO cells failed to generate any tumors despite 14 weeks of follow-up (Figure 1B). However, with continuous follow-up of mice for durations approaching one year, tumors did eventually develop in about two thirds of the HCC1569-HER3KO inoculated mice (Figure 1B). Tumors from these mice were surgically excised at necropsy for further analysis to gain insights into the mechanisms underlying the restoration of their tumorigenic properties. Tumor regrowth was not due to restoration of HER3 expression, as confirmed by western blot analysis of tumor lysates. Interestingly, we found that HER2 expression and phosphorylation were increased in HCC1569-HER3KO tumors (Figure 1C,D). This was not due to an increase in HER2 gene copy numbers as determined by FISH analysis of tumor blocks (Supplementary Figure S1C). Receptor tyrosine kinase (RTK) profiling blots were conducted on selected tumor lysates to determine whether phosphorylation of other RTKs has been induced in compensation for the loss of HER3 phosphorylation, but no such compensatory RTKs were evident besides HER2 phosphorylation (Figure 1E and Supplementary Figure S2A,S2B). To determine whether other oncogenic pathways may have supplanted the oncogene HER2, these tumors were re-implanted in mice and treated with the HER2 inhibitor lapatinib. Lapatinib inhibits the growth of these HER3-null tumors, confirming that they remain driven by HER2 (Figure 1F and Supplementary Figure S3). These HCC1569-HER3KO tumors display a lapatinib sensitivity that is nearly identical to the sensitivity of the parental HCC1569 tumors which we have previously published (11).

### **HER3-null HER2-amplified cancer cells can have active Akt signaling**

In the analysis of HER2-HER3 and downstream signaling in these tumors, it was apparent that the HCC1569-HER3KO tumors have a further increase in expression of already overexpressed HER2, accompanied by further increase in autophosphorylation of HER2, in comparison with HCC1569-HER3WT controls (Figure 1C,D). Differences in tumor cellularity were accounted for by a vimentin blot that is specific for human vimentin and non-cross reactive with mouse vimentin (confirmed in Supplementary Figure S4), making it easier to interpret the data from the low cellularity T1 tumor. With this in mind, it is evident that MAPK signaling is increased in most tumors above control cells. This could be a consequence of the observed increase in HER2 autophosphorylation. Alternatively observed increase in HER2 phosphorylation may be a consequence of a primary increase in MAPK activity, with consequential effects on HER2 trafficking or membrane stability or phosphorylation half-life. The observations with Akt signaling were more unexpected and reflects diverse mechanisms used for bypassing the requirement for HER3. Some HCC1569-HER3KO tumors show a reduction or loss of Akt signaling, expected from their lack of HER3 function which is recognized as the predominant upstream effector of Akt signaling in HER2-amplified cancers. However, other tumors have restoration of Akt signaling despite the complete absence of HER3 expression. This suggests that HER2, when overexpressed, may be competent at activating Akt in a HER3-independent manner. Akt activation in HCC1569-HER3KO cells is driven by HER2, since it is lost with lapatinib treatment (Figure 1G).



### **HER2-Akt signaling is preserved in HER3 knockdown cells**

Although the evidence from the recurrent HCC1569-HER3KO tumors shows that the requirement for HER3 can be supplanted through diverse mechanisms, the one possibility that HER2 could activate PI3K directly was intriguing and surprising, and thus we pursued a series of experiments to more directly explore this potential activity in HER2.

For this we used NR6 cells which lack the expression of the entire HER family of RTKs (confirmed in Supplementary Figure S5) (12). Stable overexpression of HER2 in NR6 cells leads to cell transformation despite the lack of HER3 or any other HER family partners in these cells (Figure 2A). These HER2-transformed cells show increased MAPK and Akt signaling compared with controls (Figure 2B,C). The increased MAPK and Akt signaling is attributable to upstream HER2 since it is suppressed by lapatinib. The increased Akt signaling is mediated through PI3K, since it is suppressed by PI3K inhibitors (Figure 2D). The activation of Akt in these cells is not due to a secondary induction of HER3 that is a consequence of HER2 transformation, as HER3 remains silent in these cells following HER2-transformation (Supplementary Figure S5). This evidence supports the hypothesis that HER2, when overexpressed, can activate Akt and induce cell transformation without a requirement for its heterodimeric partners including HER3.

Since HER2 appears capable of activating PI3K without its HER family partners, we next asked whether some of the PI3K/Akt signaling in HER2-amplified cancer cells may be directly mediated by HER2 rather than through HER3. This was done by engineering HER2-amplified cancer cell lines with doxycycline-inducible shRNA knockdown of HER3 expression. In three different examples of HER2-amplified cancer cells, it is evident that substantial Akt signaling persists despite near complete suppression of HER3 expression (Figure 2E). The observed Akt signaling in the absence of HER3 is driven by HER2, not other receptor families, as it is lost following lapatinib treatment (Figure 2E).

### **HER3-independent Akt activation does not require Ras in HER2-amplified cancer cells.**

To explore the mechanism by which HER2 mediates Akt activation in these tumor cells, we studied the contribution of the small GTPase Ras. Ras has been shown to directly interact with and activate class I PI3Ks through a Ras binding domain (RBD) that is present in the p110 catalytic subunit of PI3K (13–15). This may provide an alternative and redundant pathway linking over-expressed HER2 with PI3K which can account for the observed lapatinib-sensitive HER2-Akt signaling in HER2-amplified cancer cells. We subjected HCC1569TR-shHER3, BT474TR-shHER3, and SkBr3TR-shHER3 cells to the dox-induced depletion of HER3 and also the depletion of Ras using pooled siRNAs targeting H-Ras, N-Ras, and K-Ras. The depletion of HER3 and Ras proteins has a small effect on Akt signaling in two of these cell types, but substantial Akt signaling remains and is lapatinib-suppressible, confirming that it is driven by HER2 in these cells (Figure 3).

### **HER2 interaction with PI3K does not require partners or known adapters**

To determine whether HER2 can itself recruit and activate PI3K, we looked for the p85 regulatory subunit of PI3K in HER2 immune complexes. This interaction was studied initially in the simpler NR6 experimental cell system and subsequently in the more

physiologic cancer cell context. In HER2-transformed NR6 cells, p85 is readily detected in HER2 immune complexes, and this interaction is lost when HER2 is dephosphorylated by lapatinib treatment (Figure 4A). This interaction cannot be mediated through the HER family heterodimeric partners of HER2 as NR6 cells lack expression of the HER family proteins (Supplementary Figure S5).

The interaction was then studied in HER2-amplified cancer cells. HCC1569TR-shHER3, BT474TR-shHER3, and SkBr3TR-shHER3 cells were depleted of HER3 expression by doxycycline treatment and the presence of p85 was clearly detected in HER2 immune complexes in these cancer cells (Figure 4B). HER2-p85 interaction was also detected in HCC1569-HER3KO cells (Figure 4C). The interaction requires HER2 phosphorylation and is lost following lapatinib treatment (Figure 4A–C). The specific p85 isoform that is expressed and that is observed in HER2 immune complexes varies depending on the cell context and this was determined in an initial set of experiments (Supplementary Figure S6A).

The HER2-PI3K interaction, in these cancer cells, may in theory be indirectly mediated through the other heterodimeric partners of HER2, either EGFR or HER4. The three cancer cell lines studied above lack expression of HER4, eliminating this as an intermediate, but they do express EGFR. EGFR lacks consensus phosphotyrosine binding sites for p85, but can nevertheless bind and activate PI3K indirectly through Gab1(6,16). To address this we subjected HCC1569TR-shHER3, BT474TR-shHER3, and SkBr3TR-shHER3 cells to the dox-induced depletion of HER3 and also the siRNA induced depletion of EGFR. The interaction of p85 with HER2 was retained in these HER3 and EGFR depleted cells, again suggesting a direct interaction (Figure 5A). This interaction requires HER2 phosphorylation as it is lost upon lapatinib treatment (Figure 5A).

HER2 activates the Ras/MAPK pathway via the recruitment of the adaptor proteins Grb2 and Shc to different tyrosines located in its C-terminal tail (17,18). These adaptor proteins could potentially also be mediating the interaction with PI3K as has been shown for other tyrosine receptors kinases (19–21). To explore this possibility, we looked for those adaptor proteins in co-immunoprecipitation assays. We detected Grb2, but not Shc, in HER2 immune complexes in the three HER2-amplified cancer cell lines (Figure 5B). This interaction was also lapatinib-sensitive. To determine whether the HER2-p85 interaction was mediated through Grb2, we subjected HCC1569TR-shHER3, BT474TR-shHER3, and SkBr3TR-shHER3 cells to the dox-induced depletion of HER3 and also the siRNA induced depletion of Grb2. The depletion of HER3 and Grb2 proteins partially reduces the observed p85 protein in HER2 immune complexes in one of the three cell types (Figure 5C). But residual HER2-p85 interaction is evident nevertheless. The interaction requires phosphorylation of HER2 as it is lost following lapatinib treatment. To validate that the interaction between HER2 and PI3K occurs in a Ras-independent manner, we performed co-immunoprecipitation assays in control and Ras-depleted cells. HER2-PI3K complexes are preserved in tumor cells depleted of both HER3 and Ras proteins and these complexes remain lapatinib-sensitive (Supplementary Figure S6B).

### HER2-Akt signaling is a product of massive HER2 expression

The interaction of HER2 with PI3K is only seen in the context of constitutive phosphorylation induced by massive HER2 expression such as when experimentally overexpressed in NR6 cells, or when overexpressed due to gene amplification in cancer cells. It is important to note that this interaction is not detected in the normal physiologic setting of signaling, such as in cells with normal levels of HER2 expression that are stimulated to induce HER2-HER3 phosphorylation and signaling by physiologic ligands (Figure 5D).

### HER2-PI3K interaction requires HER2-Y1139 phosphorylation

Since the intermediaries such as Ras or Grb2 could not entirely account for the HER2-PI3K interaction, we investigated the possibility that HER2 may engage PI3K directly. The HER2 c-terminal tail has numerous tyrosines that are phosphorylated during physiologic ligand-driven receptor signaling. Some of these are also constitutively phosphorylated when HER2 is massively overexpressed such as in HER2-amplified cancer cells. In fact, the constitutive autophosphorylation of HER2 c-terminal tyrosines is increased in HER3 knockout HCC1569 cancer cells, suggesting that they may play a role in compensation for the loss of HER3 (Figure 1C and Supplementary Figure S1A). A similar upregulation of HER2 phosphorylation becomes evident in HER3 shRNA knockdown cells if the knockdown is maintained for several weeks (Supplementary Figure S7). A substantial conceptual barrier to the hypothesis that HER2 phosphotyrosines may directly engage PI3K is prior biochemical studies that have failed to identify such an interaction, and proteomic studies that have described consensus binding sites for the p85 subunit of PI3K on the c-terminal tails of HER3 and HER4, but not on HER2 (22–24). However these determinations have been made in the context of physiologic signaling and in cells with normal levels of expression of these proteins, in attempts to understand the basic mechanisms underlying cell signaling. The massive overexpression of HER2 that occurs in cancer cells may render significance to low affinity interactions that may be insignificant at normal expression levels and may have been dismissed in prior studies. In biochemical studies of peptides derived from the c-terminal tails of the HER family RTKs, the HER2 c-terminal tail indeed lacks high affinity binding sites for p85. However several peptides from sites of tyrosine phosphorylation of HER2 were found to have low affinity and Y1139 had an intermediate affinity for the SH2 domain of p85(25). Therefore we interrogated whether these tyrosines on HER2 may be mediating the observed PI3K binding and signaling observed with overexpression of HER2. These tyrosines are indeed phosphorylated in HCC1569 cells and their phosphorylation increases over time when HER3 expression is knocked down (Figure 1C, 6A and Supplementary Figure S7). Initially a quadruple YF mutant of HER2 was generated (HER2 4YF) mutated at Y1023, Y1139, Y1221, and Y1222 and was overexpressed in CHO-K1 cells which have very low expression of HER2 and lack expression of the other members of the HER family (26,27). While wildtype HER2 is observed to interact with p85 and induce the stimulation of Akt signaling above endogenous levels, this is substantially reduced in the HER2 4YF mutant (Figure 6B,6C). The p85 binding and Akt stimulation are linked with the autophosphorylation of HER2 as they are eliminated following lapatinib treatment. To more specifically interrogate the role of the 4 individual tyrosines, we generated single and various combinations of double YF mutants and expressed them in CHO-K1 cells. The stability and

expression of all these mutants was confirmed (Supplementary Figure S8). The results from co-immunoprecipitations assays using these single and double mutant constructs identify that Y1139 is the critical tyrosine for p85 binding (Figure 6D).

### NeuT-Y1143F mutation reduces transformation and tumor growth

While the data above strongly suggests the direct activation of PI3K by HER2, it does not address its functional significance. To address this, we sought to determine whether this activity of HER2 is relevant to transformation or tumorigenesis. Since mutating all the copies of the HER2 amplicon in the existing HER2-amplified cancer cell lines is not technically feasible, we tested the functional role of this tyrosine in experimental models of HER2/Neu induced transformation and tumorigenesis. MCF10A immortalized breast epithelial cells were transformed by NeuT, the rodent oncogenic homologue of HER2. The choice of NeuT over HER2 was due to its strongly transforming and tumorigenic properties in this experimental model, since human HER2 is only minimally transforming and non-tumorigenic in these epithelial cells. As such MCF10A-NeuT cells are widely used as a surrogate for the study of HER2-driven transformation (28–33). MCF10A cells were transfected with vector control, with NeuT, or with NeuT-Y1143F, the tyrosine homologous to Y1139 in human HER2 (Figure 7A) and similar expression levels of the two constructs confirmed (Figure 7B). As expected, overexpression of NeuT induces a hyperactivation of Akt, however this activity is substantially reduced in the NeuT<sup>Y1143F</sup> mutant (Figure 7B). The role of downstream signaling pathways, other than PI3K, in mediating p-Y1143 signaling is difficult to know. In soft agar colony formation assays, NeuT is highly transforming, whereas the NeuT<sup>Y1143F</sup> mutant has 40% impairment in transformation efficiency and significantly decreased acini diameter (Figure 7C,7D). The tumorigenic activity of these NeuT constructs was compared by inoculating NSG mice with these MCF10A transformed cells. Comparison of these experimental arms shows a clear impairment in the tumorigenic activity of NeuT imparted by a Y1143F mutation (Figure 7E).

### Discussion

Understanding how HER2 promotes tumorigenic growth is a subject of great interest that continues to evolve. The current state of our understanding suggests that HER3 is essential for HER2-driven tumorigenesis. This is based on HER3 knockdown studies in human cancer cell lines, and mammary ERBB3 gene ablation in a mouse genetic model of Neu-induced mammary tumorigenesis (8–10). Our findings do not refute these reports, but rather expand upon them. We confirm the suppression of tumor growth following HER3 knockout in HCC1569 cells, consistent with knockdowns reported in two other cell lines (8,9). However we report that this requirement can ultimately be overcome. The mouse mammary ERBB3 gene ablation is not directly comparable to HER3 knockout in a HER2-amplified cancer cell line since the former is a test of tumor genesis while the latter is a test of established tumors. HER3 or ERBB3 may yet have a requirement for the genesis of HER2 or Neu driven tumors that cannot be supplanted. However the requirement in the case of established tumors is clearly supplantable as we have shown.

This work highlights important features of the oncogene HER2 that sets it apart from many other kinase oncogenes. The mode by which the HER2 proto-oncogene is converted into an oncogene is through gene amplification and protein overexpression. A gain-of-function incurred by amplification and overexpression, unlike gain-of-function incurred by point mutation or fusion events, is a progressive and quantitative mode of enhancing function. Certain functions may be gained at lower thresholds of overexpression, while additional functions may be gained at higher thresholds of overexpression. It appears that the HER2 oncoprotein, at overexpression and phosphorylation levels sufficient for cellular transformation, is unable to drive tumorigenesis by itself and requires a partner in HER3. However, at higher levels of HER2 phosphorylation, the requirement for HER3 can be overcome. An increase in HER2 phosphorylation can occur through further increases in amplification levels, increases in HER2 transcription or protein half-life, increases in homodimerization events, or perhaps decreases in dephosphorylation activity. Such a volume knob attribute is not readily evident in kinase oncogenes activated through mutational events.

Quantitative functions gained through progressive increases in expression are likely to be related to increased interaction partners, conferring a degree of promiscuity to an otherwise highly specific and focused physiologic signaling network. Here we show that a weak affinity interaction between phosphorylated HER2 and PI3K becomes significant at very high expression thresholds. It is also possible that there are HER2 interactions with additional proteins that gain significance at very high expression levels, and these may also contribute to the tumorigenic properties of HER2 overexpression, including those that are redundant or non-redundant with HER3, and which may contribute to the initial HER2-induced tumorigenesis or contribute to its escape from HER3 dependency. A protein microarray study on the HER signaling network and its interacting partners performed by Jonas et al., 2006 revealed that HER3 interacting network changes very little as the affinity threshold of the interactions is lowered, whereas EGFR and HER2 become much more promiscuous (25). These data suggest that elevated levels of HER3 should primarily induce stronger signaling through pathways that are normally activated by low levels of HER3. In contrast, elevated levels of EGFR or HER2 should induce signaling through alternative pathways that are not activated at lower levels. The biological implication of this finding in the context of HER2 overexpression is profound since a large subset of breast, esophageal and gastric cancers show HER2 amplification or overexpression (34–39). It is possible that the high oncogenic potential of HER2 arises, at least in part, from its ability to turn on different pathways when overexpressed, rather than simply from stronger signaling through its primary pathways.

The repertoire of effector mechanisms engaged by HER2 may also be cell context dependent and we see evidence of this here as well. For example, the knock-down assays performed using siRNAs against Ras, EGFR and Grb2 revealed that EGFR may contribute more significantly to PI3K/Akt activation in HCC1569 cells but not in BT474 and SkBr3 cells, Ras may contribute more to PI3K/Akt activation in HCC1569 and SkBr3 and less in BT474 cells, and Grb2 may partially mediate PI3K/Akt signaling in BT474 cells but not in HCC1569 or SkBr3 cells. As such, it appears that HER2 can activate PI3K/Akt through a variety of direct and indirect effector mechanisms that may be available to it. Some tumors

in our initial series developed HER3 independency without an obvious restoration of Akt signaling (Figure 1C). Even these tumors remain driven by HER2 as evident by lapatinib treatment of one such tumor (Figure 1F and Supplementary Figure S3). The heterogeneity in effector signaling mechanisms is merely a consequence of the promiscuity that comes with massive overexpression. While such heterogeneity presents a daunting case for the selection of targeted therapies to be used in combination with HER2 inhibitors, it does portray a more singular role for HER2 as the oncogenic driver of this cancer subtype, and more promising expectations for future agents that can much more potently inactivate HER2.

## Supplementary Material

Refer to Web version on PubMed Central for supplementary material.

## Acknowledgments

This work was supported in part by grants R01CA122216 and U54CA112970 from the National Institutes of Health. ARS was supported in part by a Ramon Areces Foundation postdoctoral fellowship grant. pMSCV NeuT was kindly provided by Dr. A Goga. We thank the members of the Preclinical Therapeutics Core at UCSF Helen Diller Family Comprehensive Cancer Center, in particular Julia Malato, for instruction and support for in vivo experiments; members of the Parnassus Flow Cytometry Core for cell sorting assistance (DRC Center Grant NIH P30 DK063720); Dr. Jean-Philippe Coppe for helpful discussions and Dr. Elena Minones-Moyano for providing mouse cerebellum tissue.

Financial Support:

This work was supported in part by grants R01CA122216 and U54CA112970 from the National Institutes of Health. ARS was supported in part by a Ramon Areces Foundation postdoctoral fellowship grant.

## References

1. Ursini-Siegel J, Schade B, Cardiff RD, Muller WJ. Insights from transgenic mouse models of ERBB2-induced breast cancer. *Nat Rev Cancer* 2007;7(5):389–97. [PubMed: 17446858]
2. Moasser MM. The oncogene HER2: its signaling and transforming functions and its role in human cancer pathogenesis. *Oncogene* 2007;26:6469–87. [PubMed: 17471238]
3. Roskoski R Jr. The ErbB/HER family of protein-tyrosine kinases and cancer. *Pharmacol Res* 2014;79:34–74. [PubMed: 24269963]
4. Soltoff SP, Carraway KL 3rd, Prigent SA, Gullick WG, Cantley LC. ErbB3 is involved in activation of phosphatidylinositol 3-kinase by epidermal growth factor. *Mol Cell Biol* 1994;14(6):3550–8. [PubMed: 7515147]
5. Prigent SA, Gullick WJ. Identification of c-erbB-3 binding sites for phosphatidylinositol 3'-kinase and SHC using an EGF receptor/c-erbB-3 chimera. *EMBO J* 1994;13(12):2831–41. [PubMed: 8026468]
6. Mattoon DR, Lamothe B, Lax I, Schlessinger J. The docking protein Gab1 is the primary mediator of EGF-stimulated activation of the PI-3K/Akt cell survival pathway. *BMC Biol* 2004;2:24. [PubMed: 15550174]
7. Cohen BD, Kiener PA, Green JM, Foy L, Fell HP, Zhang K. The relationship between human epidermal growth-like factor receptor expression and cellular transformation in NIH3T3 cells. *J Biol Chem* 1996;271(48):30897–903. [PubMed: 8940074]
8. Holbro T, Beerli RR, Maurer F, Koziczak M, Barbas CF 3rd, Hynes NE. The ErbB2/ErbB3 heterodimer functions as an oncogenic unit: ErbB2 requires ErbB3 to drive breast tumor cell proliferation. *Proc Natl Acad Sci U S A* 2003;100(15):8933–8. [PubMed: 12853564]
9. Lee-Hoeflich ST, Crocker L, Yao E, Pham T, Munroe X, Hoeflich KP, et al. A central role for HER3 in HER2-amplified breast cancer: implications for targeted therapy. *Cancer Res* 2008;68(14):5878–87. [PubMed: 18632642]



10. Vaught DB, Stanford JC, Young C, Hicks DJ, Wheeler F, Rinehart C, et al. HER3 is required for HER2-induced preneoplastic changes to the breast epithelium and tumor formation. *Cancer Res* 2012;72(10):2672–82. [PubMed: 22461506]
11. Amin DN, Sergina N, Ahuja D, McMahon M, Blair JA, Wang D, et al. Resiliency and vulnerability in the HER2-HER3 tumorigenic driver. *Sci Transl Med* 2010;2(16):16ra7.
12. Pruss RM, Herschman HR. Variants of 3T3 cells lacking mitogenic response to epidermal growth factor. *Proc Natl Acad Sci U S A* 1977;74(9):3918–21. [PubMed: 302945]
13. Pacold ME, Suire S, Perisic O, Lara-Gonzalez S, Davis CT, Walker EH, et al. Crystal structure and functional analysis of Ras binding to its effector phosphoinositide 3-kinase gamma. *Cell* 2000;103(6):931–43. [PubMed: 11136978]
14. Rodriguez-Viciano P, Warne PH, Dhand R, Vanhaesebroeck B, Gout I, Fry MJ, et al. Phosphatidylinositol-3-OH kinase as a direct target of Ras. *Nature* 1994;370(6490):527–32. [PubMed: 8052307]
15. Rodriguez-Viciano P, Warne PH, Vanhaesebroeck B, Waterfield MD, Downward J. Activation of phosphoinositide 3-kinase by interaction with Ras and by point mutation. *EMBO J* 1996;15(10):2442–51. [PubMed: 8665852]
16. Sithanandam G, Smith GT, Fields JR, Fornwald LW, Anderson LM. Alternate paths from epidermal growth factor receptor to Akt in malignant versus nontransformed lung epithelial cells: ErbB3 versus Gab1. *Am J Respir Cell Mol Biol* 2005;33(5):490–9. [PubMed: 16055672]
17. Dankort D, Maslikowski B, Warner N, Kanno N, Kim H, Wang Z, et al. Grb2 and Shc adapter proteins play distinct roles in Neu (ErbB-2)-induced mammary tumorigenesis: implications for human breast cancer. *Mol Cell Biol* 2001;21(5):1540–51. [PubMed: 11238891]
18. Dankort DL, Wang Z, Blackmore V, Moran MF, Muller WJ. Distinct tyrosine autophosphorylation sites negatively and positively modulate neu-mediated transformation. *Mol Cell Biol* 1997;17(9):5410–25. [PubMed: 9271418]
19. Cully M, You H, Levine AJ, Mak TW. Beyond PTEN mutations: the PI3K pathway as an integrator of multiple inputs during tumorigenesis. *Nat Rev Cancer* 2006;6(3):184–92. [PubMed: 16453012]
20. Furge KA, Zhang YW, Vande Woude GF. Met receptor tyrosine kinase: enhanced signaling through adapter proteins. *Oncogene* 2000;19(49):5582–9. [PubMed: 11114738]
21. Radhakrishnan Y, Maile LA, Ling Y, Graves LM, Clemmons DR. Insulin-like growth factor-I stimulates Shc-dependent phosphatidylinositol 3-kinase activation via Grb2-associated p85 in vascular smooth muscle cells. *J Biol Chem* 2008;283(24):16320–31. [PubMed: 18420583]
22. Schulze WX, Deng L, Mann M. Phosphotyrosine interactome of the ErbB-receptor kinase family. *Molecular Systems Biology* 2005;doi: 10.1038/msb4100012.
23. Songyang Z, Shoelson SE, Chaudhuri M, Gish G, Pawson T, Haser WG, et al. SH2 domains recognize specific phosphopeptide sequences. *Cell* 1993;72(5):767–78. [PubMed: 7680959]
24. Piccione E, Case RD, Domchek SM, Hu P, Chaudhuri M, Backer JM, et al. Phosphatidylinositol 3-kinase p85 SH2 domain specificity defined by direct phosphopeptide/SH2 domain binding. *Biochemistry* 1993;32(13):3197–202. [PubMed: 8384875]
25. Jones RB, Gordus A, Krall JA, MacBeath G. A quantitative protein interaction network for the ErbB receptors using protein microarrays. *Nature* 2006;439(7073):168–74. [PubMed: 16273093]
26. Tzahar E, Waterman H, Chen X, Levkowitz G, Karunagaran D, Lavi S, et al. A hierarchical network of interreceptor interactions determines signal transduction by Neu differentiation factor/neuregulin and epidermal growth factor. *Molecular and Cellular Biology* 1996;16:5276–87. [PubMed: 8816440]
27. Zurita AR, Crespo PM, Koritschoner NP, Daniotti JL. Membrane distribution of epidermal growth factor receptors in cells expressing different gangliosides. *Eur J Biochem* 2004;271(12):2428–37. [PubMed: 15182358]
28. Ciardiello F, McGeady ML, Kim N, Basolo F, Hynes N, Langton BC, et al. Transforming growth factor-alpha expression is enhanced in human mammary epithelial cells transformed by an activated c-Ha-ras protooncogene but not by the c-neu protooncogene, and overexpression of the transforming growth factor-alpha complementary DNA leads to transformation. *Cell Growth Differ* 1990;1(9):407–20. [PubMed: 1981145]



29. Seton-Rogers SE, Lu Y, Hines LM, Koundinya M, LaBaer J, Muthuswamy SK, et al. Cooperation of the ErbB2 receptor and transforming growth factor beta in induction of migration and invasion in mammary epithelial cells. *Proc Natl Acad Sci U S A* 2004;101(5):1257–62. [PubMed: 14739340]
30. Giunciuglio D, Culty M, Fassina G, Masiello L, Melchiori A, Paglialunga G, et al. Invasive phenotype of MCF10A cells overexpressing c-Ha-ras and c-erbB-2 oncogenes. *Int J Cancer* 1995;63(6):815–22. [PubMed: 8847140]
31. Kim IY, Yong HY, Kang KW, Moon A. Overexpression of ErbB2 induces invasion of MCF10A human breast epithelial cells via MMP-9. *Cancer Lett* 2009;275(2):227–33. [PubMed: 19022565]
32. Qie S, Chu C, Li W, Wang C, Sang N. ErbB2 Activation Upregulates Glutaminase 1 Expression Which Promotes Breast Cancer Cell Proliferation. *Journal of cellular biochemistry* 2014;115(3): 498–509. [PubMed: 24122876]
33. Sodi VL, Khaku S, Krutilina R, Schwab LP, Vocadlo DJ, Seagroves TN, et al. mTOR/MYC Axis Regulates O-GlcNAc Transferase (OGT) Expression and O-GlcNAcylation in Breast Cancer. *Mol Cancer Res* 2015;13(5):923–33. [PubMed: 25636967]
34. Slamon DJ, Clark GM, Wong SG, Levin WJ, Ullrich A, McGuire WL. Human breast cancer: correlation of relapse and survival with amplification of the HER-2/neu oncogene. *Science* 1987;235:177–82. [PubMed: 3798106]
35. Dahlberg PS, Jacobson BA, Dahal G, Fink JM, Kratzke RA, Maddaus MA, et al. ERBB2 amplifications in esophageal adenocarcinoma. *Ann Thorac Surg* 2004;78(5):1790–800. [PubMed: 15511476]
36. Bizari L, Borim AA, Leite KR, Goncalves Fde T, Cury PM, Tajara EH, et al. Alterations of the CCND1 and HER-2/neu (ERBB2) proteins in esophageal and gastric cancers. *Cancer Genet Cytogenet* 2006;165(1):41–50. [PubMed: 16490596]
37. Saffari B, Jones LA, el-Naggar A, Felix JC, George J, Press MF. Amplification and overexpression of HER-2/neu (c-erbB2) in endometrial cancers: correlation with overall survival. *Cancer Res* 1995;55(23):5693–8. [PubMed: 7585656]
38. Junker K, Stachetzki U, Rademacher D, Linder A, Macha HN, Heinecke A, et al. HER2/neu expression and amplification in non-small cell lung cancer prior to and after neoadjuvant therapy. *Lung Cancer* 2005;48(1):59–67. [PubMed: 15777971]
39. Fajac A, Benard J, Lhomme C, Rey A, Duvillard P, Rochard F, et al. c-erbB2 gene amplification and protein expression in ovarian epithelial tumors: evaluation of their respective prognostic significance by multivariate analysis. *Int J Cancer* 1995;64(2):146–51. [PubMed: 7615357]

**Significance**

The intrinsic ability of HER2 to activate PI3K correlates with increased HER2 expression and can supplant the dependency upon HER3 for growth in HER2-amplified cancers.

Author Manuscript

Author Manuscript

Author Manuscript

Author Manuscript

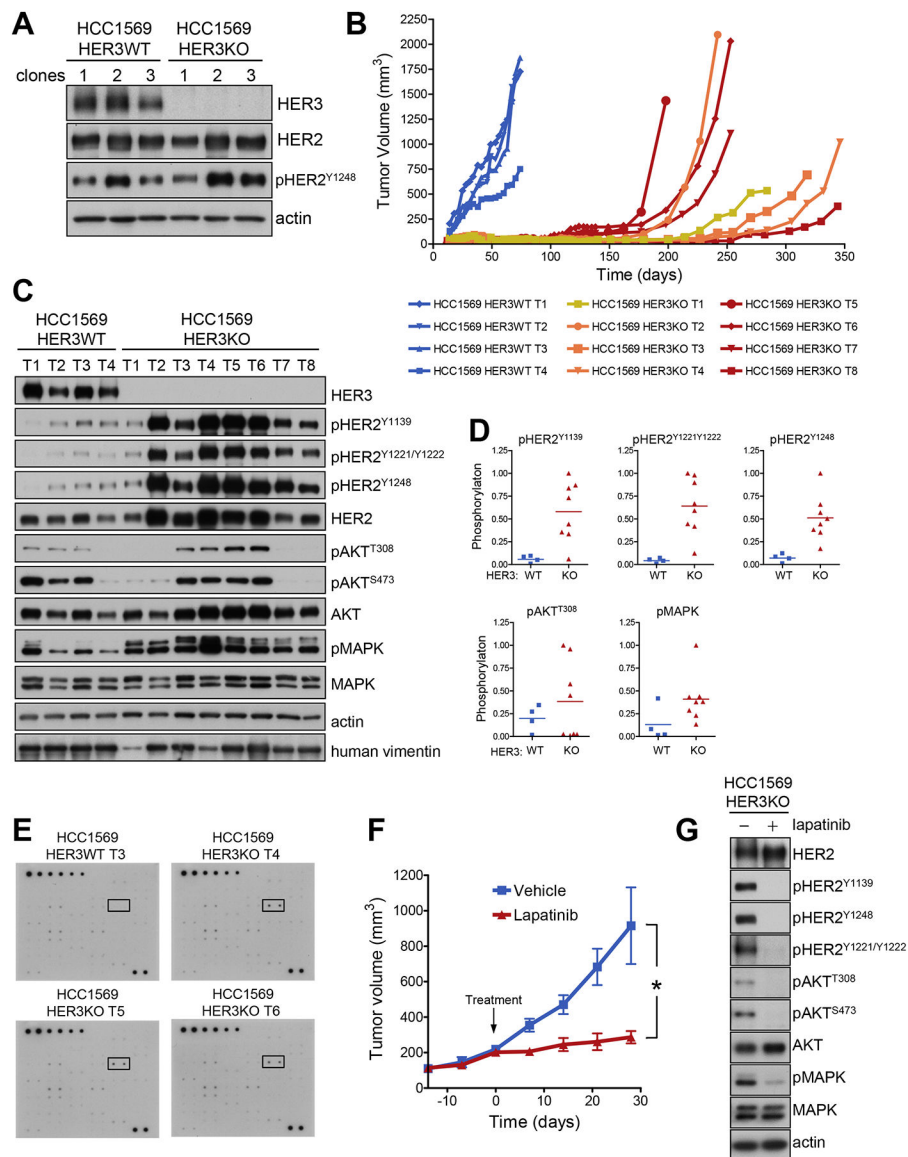


**Figure 1 – HER3 knockout in HER2-amplified cancer cells transiently suppresses tumor growth.**

HCC1569 cells underwent Crispr/Cas9 targeting of the *ERBB3* gene. Three HER3-null clones were selected for further experiments (HER3KO), and three clones that failed to undergo *ERBB3* gene targeting were selected for use as controls (HER3WT). A) Cell lysates were assayed by western blotting as indicated showing the loss of HER3 protein expression in the three HER3KO selected clones. B) Three clones from HCC1569-HER3WT and three clones from HCC1569-HER3KO cells were implanted subcutaneously into female nude mice (5 nude mice/clone;  $2 \times 10^6$  cell/implant) and tumor volume was measured weekly. The different clones of HCC1569-HER3KO cells are shown in three different colors. C) Lysates from resected tumors were immunoblotted using antibodies against the indicated proteins. The species specificity of the anti-human vimentin was confirmed in Supplementary Figure S4. D) The immunoblot signals from part C were quantified and the relative levels of pHER2, pAkt and pMAPK are shown here as indicated. Levels were normalized to actin. E)

Lysates from a HCC1569-HER3WT tumor and three HCC1569-HER3KO tumors were assayed using a phospho-RTK profiling antibody array. The array legend is provided in Supplementary Figure S2A. The rectangles indicate the duplicate dots corresponding to p-HER2. F) An HCC1569-HER3KO tumor was resected and re-implanted in 10 nude mice. When tumors reached a volume of 200mm<sup>3</sup>, HCC1569-HER3KO-bearing mice were treated daily by oral gavage either with lapatinib at 100mg/kg/day (n=5 mice) or vehicle control (n=5 mice) and tumor volumes were measured weekly. Mean tumor volumes are plotted with error bars showing SEM. The growth inhibition by lapatinib is significant at p<0.01. G) HCC1569-HER3KO cells growing in culture were treated with 1uM lapatinib or DMSO for 2 hours and cell lysates studied by western blotting as indicated.

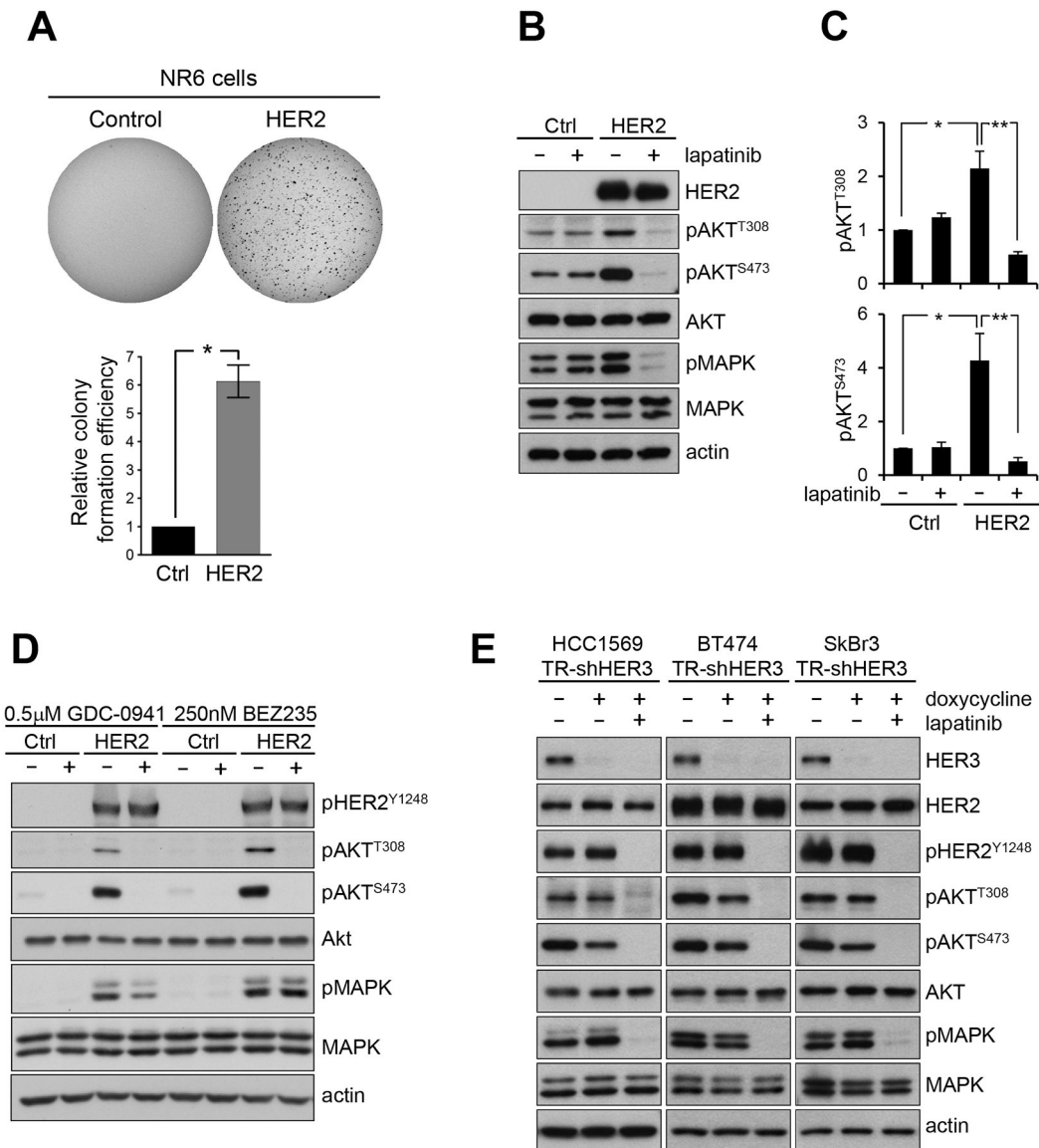


**Figure 2 – HER2 overexpression activates Akt without a requirement for HER3.**

A) NR6 cells stably transfected with HER2 or vector control were seeded in soft agar and colonies imaged and counted at 21 days. n=3 \**p*<0.03. B) Control and HER2-transfected NR6 cells were treated with 1μM lapatinib for 2h and cell lysates were assayed by western blotting as indicated. C) quantitation of pAkt signaling from the western blots of part C. Data were pooled from 3 (pAkt<sup>T308</sup>) and 5 (pAkt<sup>S473</sup>) independent experiments and are presented as the mean + SEM. \**p*<0.03; \*\**p*<0.01. D) Control and HER2-transfected NR6 cells were treated with 0.5μM GDC-0941 and 0.25μM BEZ235 for 1 hour and cell lysates were assayed by western blotting as indicated. E) HER2-overexpressing HCC1569, BT474 and SkBr3 cells engineered to induce expression of a HER3 shRNA in a dox-inducible manner were treated with 100 ng/ml doxycycline for 72h (HCC1569 and BT474) or 7 days (SkBr3) and also with 1μM lapatinib for 2 hours before cell harvest. Cell lysates were assayed by western blotting as indicated.

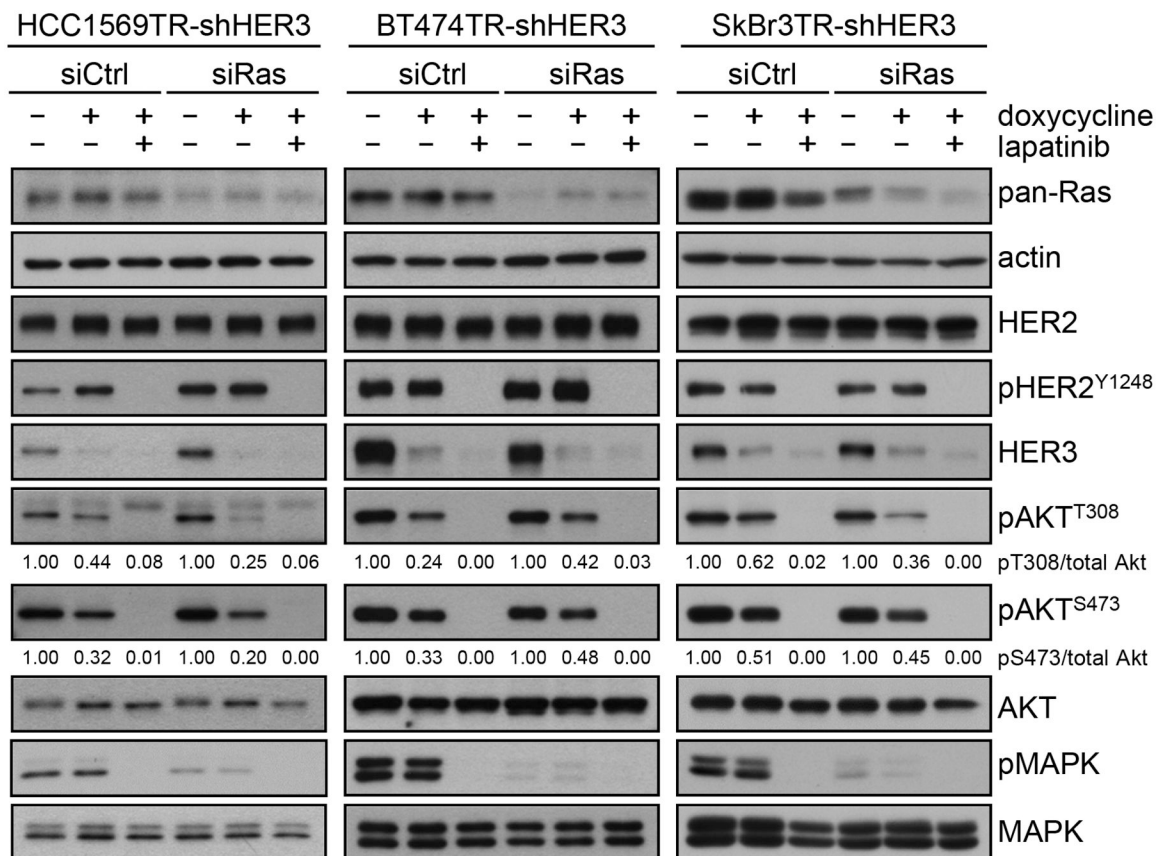


**Figure 3 –. HER2 activation of Akt does not require Ras**

A) The indicated three engineered HER2-amplified cancer cell lines were treated with 100 ng/ml doxycycline for 72h (HCC1569 and BT474) or 7 days (SkBr3) to knock down HER3 expression, and transfected with a pool of siRNA Ctrl or a pool of siRNA against H-Ras, K-Ras and N-Ras for 72h. Additional arms were also treated with 1uM lapatinib for 2h before cell harvest. Cell lysates were assayed by western blotting as indicated. Values represent the intensities of pAkt bands relative to that of the corresponding total Akt band. The blots are representative of multiple independent experiments.

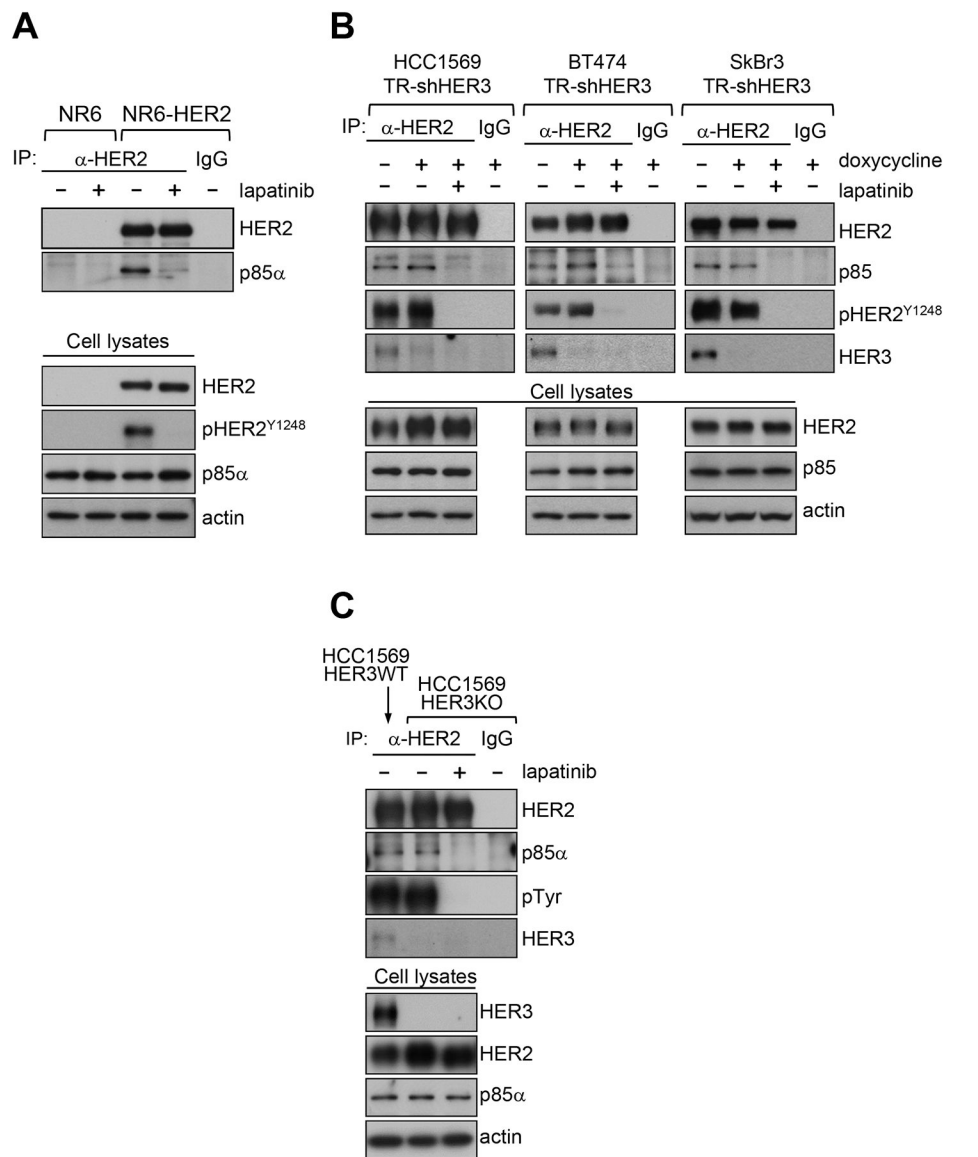


**Figure 4 – Overexpressed HER2 can bind PI3K**

A) Control and HER2-overexpressing NR6 cells were treated with 1 $\mu$ M lapatinib for 2 hours. Cell extracts were immunoprecipitated with anti-HER2 antibodies or control IgG. The immune complexes were analyzed by immunoblotting as indicated. B) The indicated HER2-amplified cancer cell lines were treated with 100 ng/ml doxycycline for 72h (HCC1569 and BT474) or 7 days (SkBr3) to knock down HER3 expression. Additional arms were also treated with 1 $\mu$ M lapatinib for 2 hours before harvest. Anti-HER2 immunoprecipitates were immunoblotted as indicated. The p85 immunoblots are specifically p85 $\alpha$  for HCC1569 and BT474 and p85 $\beta$  for SkBr3. C) HCC1569-HER3WT and HCC1569-HER3KO cells were treated with 1  $\mu$ M lapatinib for 2 hours and anti-HER2 immunoprecipitates were immunoblotted as indicated.



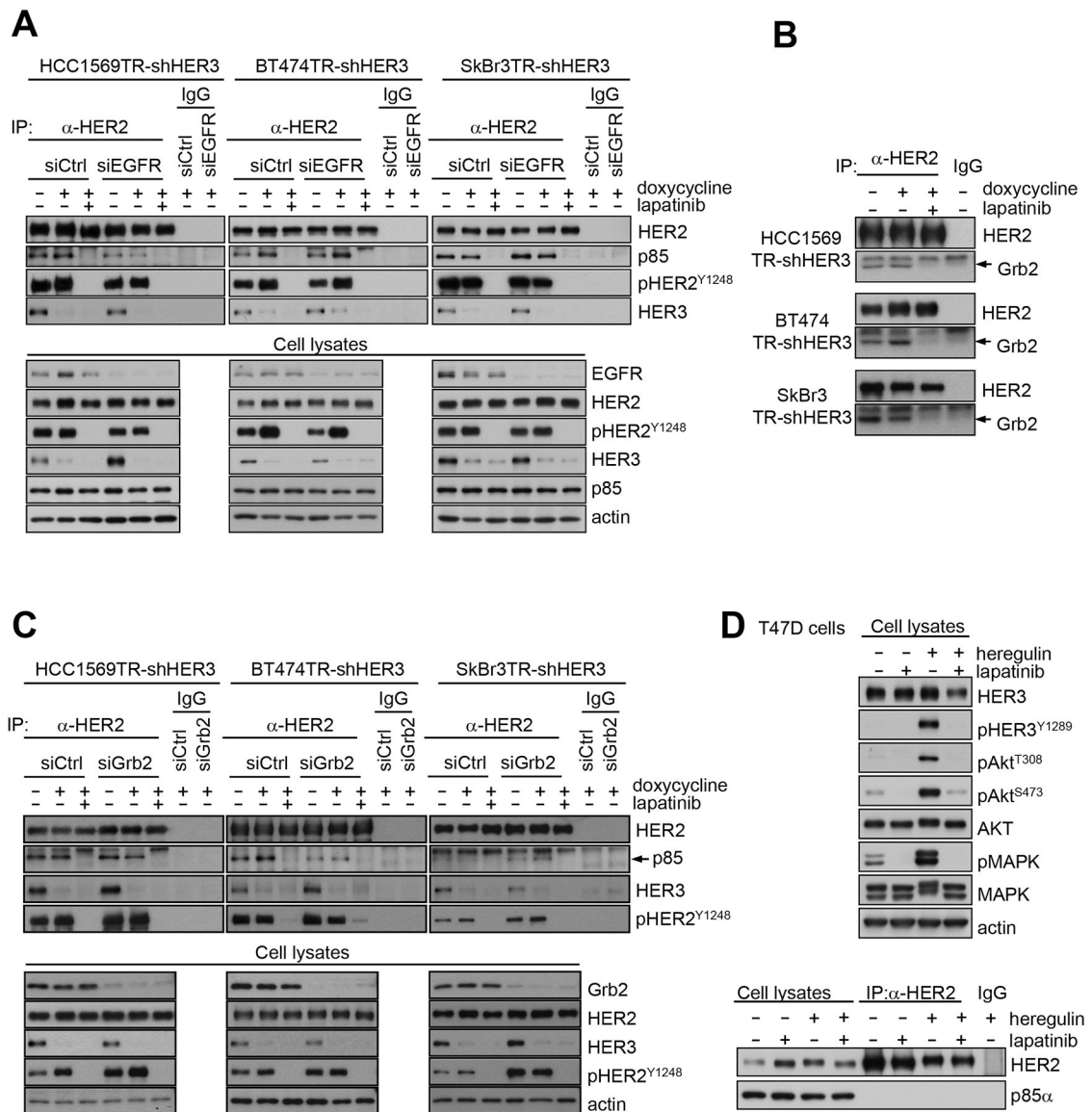


**Figure 5 – HER2 interaction with PI3K is not dependent on indirect binding partners**

A) The indicated three engineered HER2-amplified cancer cell lines were treated with 100 ng/ml doxycycline for 72h (HCC1569 and BT474) or 7 days (SkBr3) to knock down HER3 expression, and transfected with a pool of siRNA Ctrl or a pool of siRNA against EGFR for 72 hours. Additional arms were also treated with 1 $\mu$ M lapatinib for 2 hours before cell harvest. Anti-HER2 immunoprecipitates were assayed by western blotting as indicated. The p85 immunoblots are specifically p85 $\alpha$  for HCC1569 and BT474 and p85 $\beta$  for SkBr3. B) The same cell lines were depleted of HER3 expression by doxycycline treatment and anti-HER2 immunoprecipitates were assayed by western blotting for the presence of Grb2. Additional arms were also treated with 1 $\mu$ M lapatinib for 2 hours before cell harvest. C) The same cell lines were depleted of HER3 expression by doxycycline treatment and transfected with a pool of siRNA Ctrl or a pool of siRNA against Grb2 for 72 hrs. Additional arms were also treated with 1 $\mu$ M lapatinib for 2 hours before cell harvest. Anti-HER2

immunoprecipitates were assayed by western blotting as indicated. The p85 immunoblots are specifically p85 $\alpha$  for HCC1569 and BT474 and p85 $\beta$  for SkBr3. D) T47D breast cancer cells were treated with 1 $\mu$ M lapatinib for 2 hours and stimulated with 10ng/ml heregulin for 15 minutes. Cell lysates were analyzed by immuno-blotting as indicated (upper panel) or immunoprecipitated with control IgG or anti-HER2 antibodies (lower panel). The immunoprecipitates were analyzed by immuno-blotting with anti-HER2 and anti-p85 antibodies as indicated.

Author Manuscript

Author Manuscript

Author Manuscript

Author Manuscript

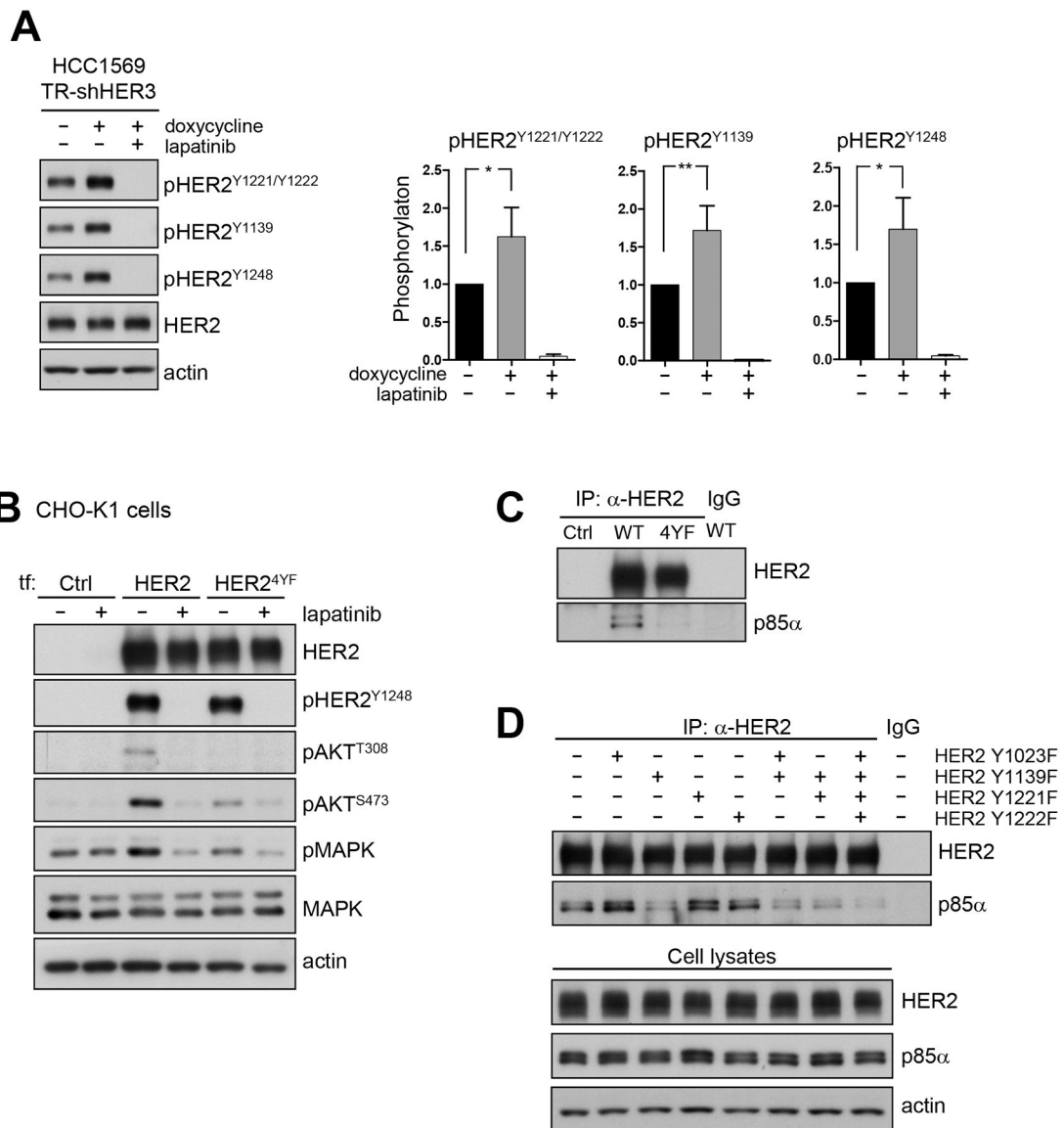


**Figure 6 – HER2 interaction with PI3K is mediated through tyr1139**

A) HCC1569TR-shHER3 cells were treated with 100 ng/ml doxycycline for 72 hours to knock down HER3 expression and the phosphorylation of HER2 c-terminal tail tyrosine residues was assayed by western blotting using the indicated antibodies. An additional arm was treated with 1μM lapatinib for 2 hours prior to harvest. The p-HER2 bands were quantified by densitometry and graphically depicted (n=4) \*, p<0.03; \*\*, p<0.01. B) CHO-K1 cells co-transfected with wildtype HER2 or a 4YF mutant of HER2 or vector control, as well as human p85α and treated with 5 μM lapatinib for 1.5h, and cell lysates analyzed by western blotting as indicated. C) CHO-K1 cells were co-transfected with wildtype HER2 or a 4YF mutant of HER2 or vector control, as well as human p85α and anti-HER2 immunoprecipitates analyzed by anti-p85α immunoblotting. D) CHO-K1 cells were co-transfected with HER2 or each of 7 different mutant-HER2 constructs as well as human p85α. Anti-HER2 immunoprecipitates were analyzed by immunoblotting as indicated.

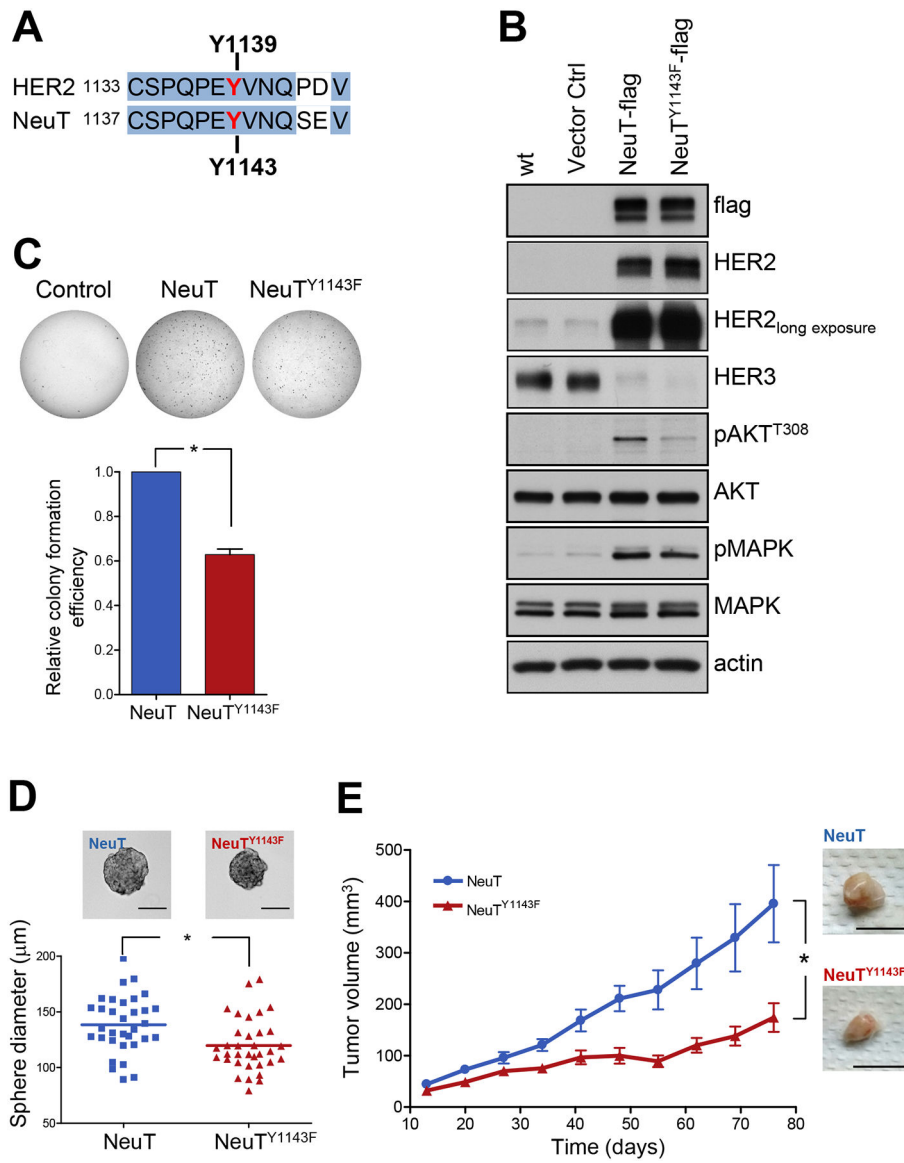


**Figure 7 –. The direct activation of PI3K by HER2/Neu contributes to tumorigenic activity**  
 A) Human and mouse sequences showing the homology between human Y1139 and mouse Y1143 in the HER2 c-terminal tail. B) MCF10A cells stably expressing flag-tagged NeuT or NeuT<sup>Y1143F</sup> were generated and immunoblotted as indicated. C-D) MCF10A-Ctrl, MCF10A-NeuT and MCF10A-NeuT<sup>Y1143F</sup> cells were seeded in soft agar and colonies imaged, counted, and colony diameters measured after 10 days. The differences in number of colonies (\*,  $p < 0.01$ ) and colony diameters (\*,  $p < 0.01$ ) are significant. Bars, 100  $\mu\text{m}$ . E) NSG mice were injected with MCF10A cells stably expressing NeuT-Flag ( $n=11$ ) or NeuT-Y<sup>1143F</sup>-Flag ( $n=10$ ) in the mammary fat pad and tumor growth was measured weekly. Mean tumor volumes are shown with standard error of the mean (\*,  $p < 0.016$ ). Representative macroscopic images of isolated tumors showing the difference in size. Bars, 1cm.